

Size-dependent deformation in nanograins and nanotwins

Pei Gu^{1,a)} and Ming Dao²

¹MSC Software Corporation, 6050 Scripps St, San Diego, California 92122, USA

²Department of Materials Science and Engineering, Massachusetts Institute of Technology, Cambridge, Massachusetts 02139, USA

(Received 4 January 2013; accepted 22 February 2013; published online 5 March 2013)

This paper discusses three aspects that have not been looked into within mechanistic model for rationalizing observed behavior of nanocrystalline materials. (1) For the nano-materials with low energy barrier to emit the trailing partial after the leading partial, such as nanocrystalline Al (nc-Al), both partials extend intra-granularly in strengthening effect. (2) In the transition grain-size region between strengthening and softening, the coupled effect of intra-granular dislocation extension and grain boundary deformation contributes to flow stress. (3) Reformulating the non-homogeneous nucleation model, the activation volume is further examined. © 2013 American Institute of Physics. [<http://dx.doi.org/10.1063/1.4794539>]

A unified mechanistic model to rationalize size-dependent flow stress, activation volume, and strain-rate sensitivity for face centered cubic (FCC) metals with either nanocrystalline (nc) grains or nanotwinned (nt) grains was proposed in our previous work.¹ The three important nano-scaled parameters are theoretically modeled by non-homogeneous dislocation nucleation and intra-granular or intra-twin dislocation extension.¹⁻⁶ Here, we continue the investigation, in particular, in three cases that have not been looked into within the mechanistic model. (1) The trailing partial is emitted into the grain following the leading partial's emission, when the energy barrier for such process is low, such that two partials with a band of stacking fault propagate intra-granularly for strengthening. (2) For small grain size, where both intra-granular dislocation extension and grain boundary deformation operate, the coupled effect of both contributes to strength softening. (3) Simplifying the non-homogeneous nucleation model, we further examine the activation volume.

Both nanocrystalline grains and nanotwins embedded in ultrafine grains are effective to enhance the mechanical strength of FCC metals.^{7,8} Dislocation cells, which can block dislocation extension, are not expected to operate in nanograins⁹ and also nanotwins, and partial dislocation extension leads to the enhancement of mechanical strength.^{1-6,10,11} In the non-uniform partial dislocation extension model,^{1,4,5} the flow stress for nanograins is expressed as

$$\tau_1 = \frac{\Gamma}{b} + G \left(\frac{1}{3} - \frac{1}{12\pi\beta} \right) \frac{b}{d}. \quad (1)$$

Here, d is the grain size, b is the magnitude of Burgers vector, Γ is the stacking fault energy, and G is the shear modulus. The normalized extension distance $\beta = (1/d^2) \int_0^d \delta(x) dx$, where $\delta(x)$ is the extension distance from the grain boundary. The flow stress model in Eq. (1) is shown in Figure 1, as marked by the strengthening portion, versus experiment data for nanocrystalline Cu (nc-Cu) from Weertman's group.¹² This comparison using different

experimental data for nc-Cu from those used in our previous work again shows appropriate model prediction. For nanocrystalline Ni (nc-Ni), the comparison of prediction with experiment data¹³⁻¹⁷ is shown in Figure 2.

For nanotwins, the flow stress is dependent of both twin thickness and grain size¹ and is expressed from the non-uniform partial dislocation extension model as

$$\tau = \frac{\Gamma}{b} + \frac{G}{2} \left(\frac{1}{3} - \frac{1}{12\pi\beta_1} \right) \frac{b}{\lambda} + \frac{G}{2} \left(\frac{1}{3} - \frac{1}{12\pi\beta_2} \right) \frac{b}{d}. \quad (2)$$

Here, λ is the twin thickness. The two normalized extension distances $\beta_1 = 1/(\lambda d) \int_0^d \delta_1(x) dx$ and $\beta_2 = 1/(\lambda d) \int_0^{\lambda} \delta_2(x) dx$, where $\delta_1(x)$ and $\delta_2(x)$ are the extension distances along the short edge and the long edge of the lamella slip plane, respectively. The flow stress model in Eq. (2) is shown in Figure 3, as marked by the strengthening portion, versus experiment data for nanotwinned Cu (nt-Cu) from Lu's

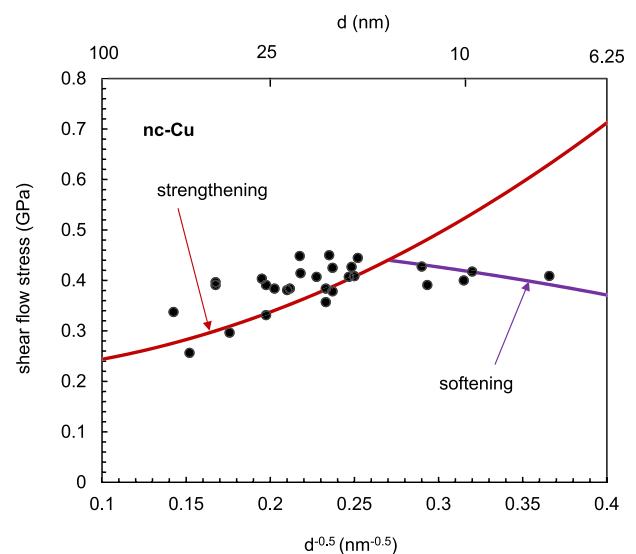


FIG. 1. Prediction of flow stress for nc-Cu: strengthening at large grain size (left side, plotted with Eq. (1)); softening at small grain size (right side, plotted with Eq. (6)). The experimental data are converted from the hardness measurements in Ref. 12.

^{a)}Email: pei.gu@mscsoftware.com.

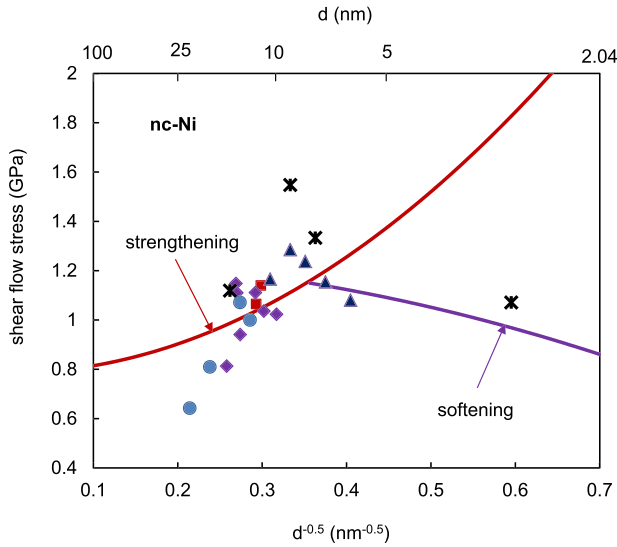


FIG. 2. Prediction of flow stress for nc-Ni. For experimental data, star symbols are from Ref. 13, triangle symbols from Ref. 14, circle symbols from Ref. 15, diamond symbols from Ref. 16, and square symbols from Ref. 17.

group.¹⁸ By choosing the extension parameters, β , β_1 , and β_2 , as specific functions of the grain size or twin thickness,¹ Eqs. (1) and (2) are equivalent to the Hall-Petch relation.

Equation (1) is derived for the situation where only the leading partial is emitted to glide intra-granularly while the trailing partial remains at the grain boundary. For nano-materials with high energy barrier for emitting the trailing partial (the ratio of unstable stacking fault energy to stacking fault energy is large), such as nc-Cu and nc-Ni, molecular dynamic (MD) simulation shows the situation without emitting trailing partial is true,¹⁰ and the prediction of Eq. (1) is in agreement with experimental data.^{1,4,5} For nano-materials with the low energy barrier, such as nc-Al, MD shows that the trailing partial is emitted following the leading partial such that a perfect dislocation, or the two partials with a band of stacking fault, extends inside the grain.^{19,20} To treat

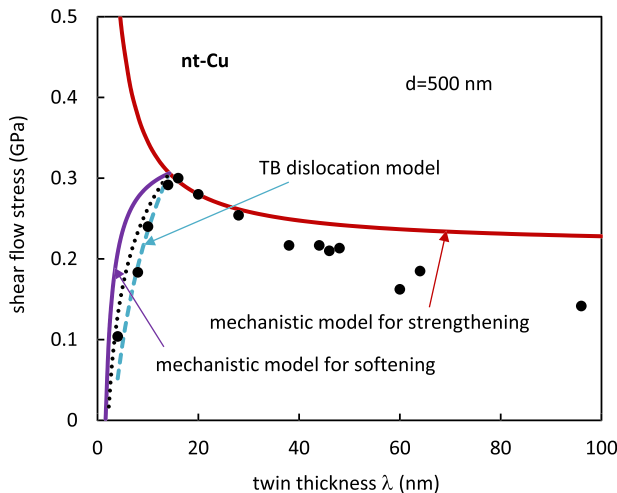


FIG. 3. Prediction of flow stress for nt-Cu: strengthening (right side, plotted with Eq. (2)); softening (left side, plotted with the developed softening model for nanotwins). The experimental data are from Ref. 18. The twin boundary (TB) dislocation softening model is plotted in dashed line. The average of the two softening models is in dotted line.

this case where both partials contribute to strengthening, we modify the free energy in Ref. 3

$$E = -\frac{Gdb^2}{12\pi} \ln \frac{\delta - s}{r_0} - T_1 d(\delta - r_0) - T_2 d(s - r_0) + \gamma d(\delta - s) + 2L_p(\delta - s) + 2L_f s. \quad (3)$$

Here, δ and s are the distances traveled by the leading and trailing partials, respectively ($\delta > s$); r_0 is the core cut-off radius; $T_1 = \tau_{ms} b_s^{(1)} + \tau_{mz} b_z^{(1)}$; and $T_2 = \tau_{ms} b_s^{(2)} + \tau_{mz} b_z^{(2)}$, where m-s-z is a coordinate system with m axis perpendicular to the slip plane and z axis along the gliding direction, and $b_i^{(1)}$ and $b_i^{(2)}$ are components of the Burgers vectors of the leading and trailing partials, respectively; the energy per unit length of a partial dislocation $L_p = Gb^2/6$; the energy per unit length of a perfect dislocation $L_f = Gb^2/2$. The first term on the right side is the interaction energy between the two partials, and the last two terms represent the side segments' energies. For acting shear stress, when both partials extend, we have $\tau b = T_1 + T_2$. When the leading partial extends and the trailing partial does not (s does not change), the trailing partial is inactive such that $\tau = T_1/b$, which with Eq. (3) and $\partial E/\partial \delta = 0$ gives Eq. (1) for the required shear stress to extend the leading partial. The definition of the extension parameter for the two partial case is $\beta = (1/d^2) \int_0^d [\delta(x) - s(x)] dx$. When the trailing partial extends and the leading partial does not (δ does not change), the leading partial is inactive such that $\tau = T_2/b$, which with Eq. (3) and $\partial E/\partial s = 0$ gives the required shear stress to extend the trailing partial

$$\tau_2 = G \left(\frac{2}{3} + \frac{1}{12\pi\beta} \right) \frac{b}{d} - \frac{\gamma}{b}. \quad (4)$$

When both partials extend, the stacking fault band's width remains as a constant $\eta = \delta - s$. Using this relation in Eq. (3) and $\partial E/\partial s = 0$, the required shear stress to extend both partials is

$$\tau_3 = G \frac{b}{d}, \quad (5)$$

which is the same as the traditional perfect dislocation extension model. A coefficient was introduced into the right side of Eq. (5) to account for the curvature of the extended dislocation loop.⁵

The flow stress is the smallest of the shear stresses given by Eqs. (1) and (5). Equation (4) does not give flow stress even if it is the smallest, since the leading partial has to be emitted first and thus in such case, the leading partial's extension or both partials' extension gives flow stress. For nc-Al, we take $b = 0.25$ nm, $G = 35$ GPa, and $\gamma = 0.146$ J/m². The calculation using representative β values shows that Eq. (5) gives flow stress for $d > 14$ nm; otherwise, Eq. (1) gives flow stress. In other words, except for very small grain size, a perfect dislocation, or both partials with a band of stacking fault, propagates. The prediction from the model versus available experimental data^{21,22} for nc-Al is shown in Figure 4.

It is noted that taking $L_f = Gb^2/2$ and $L_p = Gb^2/6$ for the side segments in deriving the required stresses is an approximation; therefore β obtained by fitting experimental

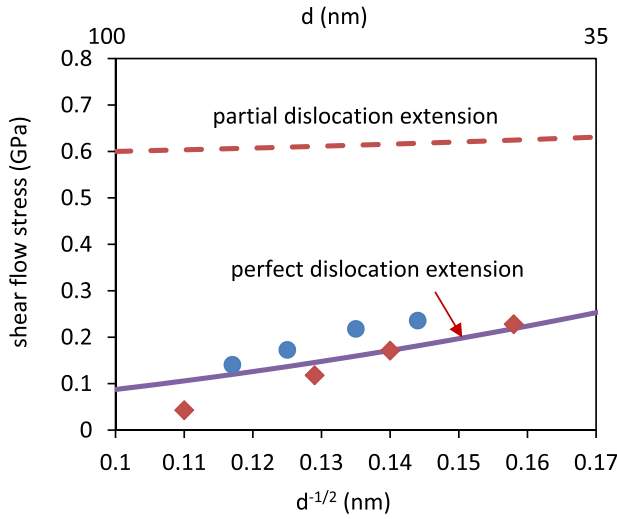


FIG. 4. Prediction of flow stress for nc-Al with Eq. (5). For experimental data, circle symbols are from Ref. 21, and diamond symbols are from Ref. 22.

data is a reference value for extension distance. Accurately modeling the side segment's energy would require the consideration of the grain boundary structure. However, the grain-size dependent terms in Eqs. (1), (4), and (5) represent the competition of side segments and interior segment in strengthening nanograins.

When the grain size becomes very small, strength softening occurs where with decreased grain size, the strength decreases.^{12,23} MD simulation shows such softening is ascribed to grain boundary deformation mechanism;^{10,24} analytical models through grain boundary sliding and diffusion were proposed, where physical based relation, such as that between shear strain rate of grain boundary and required shear stress, was employed.^{23,25–27} At large grain size intra-granular dislocation operates for strengthening; at very small grain size grain boundary deformation becomes dominate. In the transition region in-between, or even in a smaller grain size below this region, MD simulation reveals the evidence of coexistence of intra-granular dislocations and grain boundary sliding.^{19,28} Here, we extend the above flow stress model to probe the contribution of intra-granular dislocations to softening in the assistance of grain boundary deformation. For this, we consider that when the grain boundary is increasingly active as the grain size becomes smaller, side segments of the intra-granular dislocation loop annihilate into the grain boundary. Due to the annihilation, the interior segment extends without the constraint of the side segments, and thus the side segments' contribution to the flow stress is removed from Eq. (1) such that the reference shear stress for this state is $\tau_0 = \Gamma/b - G/(12\pi)b/d$. Considering the rate-dependent deformation nature of grain boundary deformation, the required shear stress for strength softening in the region of small grain size is written as

$$\tau = C\tau_0\dot{\gamma}^m \equiv C\left[\frac{\Gamma}{b} - \frac{Gb}{12\pi d}\right]\dot{\gamma}^m. \quad (6)$$

Here, the strain rate sensitivity m represents the nature of the strain rate dependence on the grain boundary deformation. The scaling factor C is obtained from equating Eq. (6)

with Eq. (1) at the critical grain size for strength softening, measured through experiment, and at the strain rate where the experiment is conducted. The reference shear stress τ_0 is the flow stress at $C\dot{\gamma}_0^m = 1$. The prediction of softening portions is shown in Figures 1 and 2 for nc-Cu and nc-Ni. For nanotwins, softening at small twin thickness was also observed¹⁸ and modeled via twin boundary dislocations²⁹ and Lomer dislocations.³⁰ Similar discussion as above is done for nanotwins where the side segments of the intra-twin dislocation loop extending toward the twin boundary are annihilated into the grain boundary. The flow stress for strength softening in nanotwins is given by $\tau = C[\Gamma/b - G/(12\pi)b/\lambda]\dot{\gamma}^m$ (we consider $d \gg \lambda$). The prediction for the softening portion of nt-Cu is plotted in Figure 3, together with that from the twin boundary dislocation model.²⁹

The grain size and/or twin thickness dependent activation size of nanostructures is determined from the non-homogeneous dislocation nucleation model¹ in which the free energy is

$$E = \frac{5}{16}Gb_1^2r \ln \frac{r}{r_0} - \frac{1}{2}C_f\tau b_1\pi(r^2 - r_0^2) + \frac{1}{2}\gamma\pi(r^2 - r_0^2). \quad (7)$$

Here, τ is the flow stress; C_f is the stress concentration factor at the nucleation site; r is the dislocation loop radius; $b_1 = b/\sqrt{3}$; $r_0 = b_1$. Maximizing the free energy gives the activation loop radius

$$r_c = \alpha \left(\frac{\tau}{G} - \frac{\gamma}{C_f G b_1} \right)^{-1} b \left(\ln \frac{r_c}{r_0} + 1 \right). \quad (8)$$

Here, $\alpha = 5/(16\pi C_f \sqrt{3})$. The activation volume $V = \pi r_c^2 b/2$. We make two assumptions for Eq. (8) to simplify it. First, α values obtained in Ref. 1 in fitting experimental data indicate $C_f \gg 1$. Due to this, $\gamma/(C_f G b_1)$ is much smaller than τ/G such that the former is neglected. Second, avoiding treating the logarithm function, we expand it into series: $\ln x = \sum_{k=1}^{\infty} (1/k)(1 - 1/x)^k$, in which we ignore any non-linear terms ($k > 1$) and also $1/x$ in the linear term, considering $x > 1$. Using these simplifications, we obtain from Eq. (8)

$$V = 2\pi\alpha^2 \left(\frac{G}{\tau} \right)^2 b^3. \quad (9)$$

Rearranging Eq. (9), flow stress is expressed in terms of activation volume as $\tau = \sqrt{2\pi\alpha G b \sqrt{b/V}}$. Note that b/V bears the unit of dislocation density. For microcrystalline materials, it was shown that flow stress is proportional to $\sqrt{\rho}$, where ρ represents dislocation density ($\rho \sim b^4/V^2$).³¹

We express the grain-size dependence of activation volume explicitly. For this, Eq. (1) is substituted into Eq. (9), and after rearrangement, we obtain

$$\frac{1}{2\pi\alpha^2} \left(\frac{\gamma}{Gb} \right)^2 + \frac{1}{\pi\alpha^2} \frac{\gamma}{Gb} \left(\frac{1}{3} - \frac{1}{12\pi\beta} \right) \frac{b}{d} + \frac{1}{2\pi\alpha^2} \left(\frac{1}{3} - \frac{1}{12\pi\beta} \right)^2 \left(\frac{b}{d} \right)^2 = \frac{b^3}{V}. \quad (10)$$

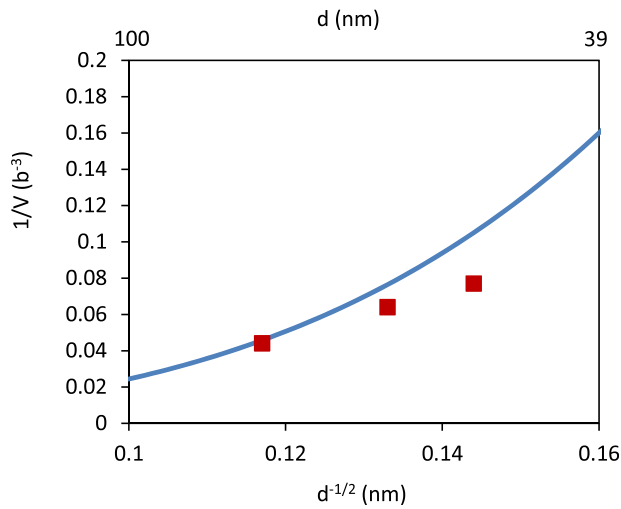


FIG. 5. Prediction of activation volume for nc-Al versus experimental data from Ref. 21.

Considering $d \gg b$ such that the third term on the left side of Eq. (10), second order term, is neglected, and using the relation between the extension parameter β and the Hall-Petch slope for flow stress K_1 , given in Ref. 1, we obtain the Hall-Petch type relation for activation volume

$$\frac{1}{2\pi\alpha^2} \left(\frac{\gamma}{Gb} \right)^2 + \frac{1}{\pi\alpha^2} \frac{\gamma K_1}{Gb G} \frac{1}{\sqrt{d}} = \frac{b^3}{V}. \quad (11)$$

Similar Hall-Petch type relations for activation volume were derived from dislocation pileup against grain boundary.^{32–34} In their formulations, two parameters were introduced, one for grain interior activation and another for grain boundary activation; in the above formulation, only one parameter α is defined for stress concentration at the nucleation site. With appropriate α , Eqs. (10) and (11) compare satisfactorily to the experimental data of nc-Cu (Figure 5 in Ref. 1). For other nanograined materials, size-dependent experimental data for activation volume are limited, and the material properties given in Ref. 5 are used in Eq. (10) for prediction. When $d = 30$ nm and $C_f = 5$, $V = 6.2b^3$ for nc-Ni, which is consistent with the experimental data $10b^3$.³⁵ When $d = 10$ nm and $C_f = 10$, $V = 2.6b^3$ for nanocrystalline Pd (nc-Pd), which is consistent with the experimental data $4b^3$.³⁶ The strain-rate sensitivity calculated from its definition^{1,3} for the nc-Ni and nc-Pd is also in agreement in the magnitude order with experimental data.^{35–37}

For nc-Al, we substitute Eq. (5) for perfect dislocation extension into Eq. (9) to obtain

$$V = 2\pi\alpha^2 d^2 b, \quad (12)$$

which, with $C_f = 10$, compares well in Figure 5 with experimental data from Ref. 21. The strain-rate sensitivity obtained from its definition, $m = \sqrt{3kT}/(4\pi\alpha^2 Gdb^2)$, where T is absolute temperature and k is Boltzmann constant, is comparable with experimental data in Ref. 21. In addition, the magnitude order of the activation volume and strain-rate sensitivity calculated in this way is consistent with experiment measurement for nc-Al in Ref. 38 (although grain growth was observed there). From the definition of α and

Eq. (9), it is seen that the activation volume is inversely proportional to C_f^2 such that it is sensitive to the stress concentration at the nucleation site. The Hall-Petch type relation for activation volume of nanotwins can be obtained by substituting Eq. (2) into Eq. (9).

In summary, from mechanistic modeling approach, we investigate the intra-granular extension of trailing partial due to the low energy barrier for its emission; the coupled deformation of intra-granular dislocation and grain boundary in contributing to flow stress; and the simplified version of non-homogeneous nucleation model. Continuing our previous work, these modeling efforts elucidate intra-granular dislocations and their interaction with non-homogeneous sources such as grain boundaries in nano-strengthening process.

- ¹P. Gu, M. Dao, R. J. Asaro, and S. Suresh, *Acta Mater.* **59**, 6861 (2011).
- ²R. J. Asaro, P. Krysl, and B. Kad, *Philos. Mag. Lett.* **83**, 733 (2003).
- ³R. J. Asaro and S. Suresh, *Acta Mater.* **53**, 3369 (2005).
- ⁴P. Gu, B. Kad, and M. Dao, *Scr. Mater.* **62**, 361 (2010).
- ⁵P. Gu, B. Kad, and M. Dao, *Philos. Mag. Lett.* **92**, 111 (2012).
- ⁶R. J. Asaro and Y. Kulkarni, *Scr. Mater.* **58**, 389 (2008).
- ⁷M. A. Meyers, A. Mishra, and D. J. Benson, *Prog. Mater. Sci.* **51**, 427 (2006).
- ⁸M. Dao, L. Lu, R. J. Asaro, J. T. M. De Hosson, and E. Ma, *Acta Mater.* **55**, 4041 (2007).
- ⁹H. Conrad, *Metall. Mater. Trans. A* **35**, 2681 (2004).
- ¹⁰H. Van Swygenhoven, M. Spaczer, and A. Caro, *Acta Mater.* **47**, 3117 (1999).
- ¹¹X. Z. Liao, S. G. Srinivasan, Y. H. Zhao, M. I. Baskes, Y. T. Zhu, F. Zhou, E. J. Lavernia, and H. F. Xu, *Appl. Phys. Lett.* **84**, 3564 (2004).
- ¹²P. G. Sanders, J. A. Eastman, and J. R. Weertman, *Acta Mater.* **45**, 4019 (1997).
- ¹³T. Yamasaki, *Scr. Mater.* **44**, 1497 (2001).
- ¹⁴C. A. Schuh, T. G. Nieh, and H. Iwasaki, *Acta Mater.* **51**, 431 (2003).
- ¹⁵C. A. Schuh, T. G. Nieh, and T. Yamasaki, *Scr. Mater.* **46**, 735 (2002).
- ¹⁶A. F. Zimmerman, G. Palumbo, K. T. Aust, and U. Erb, *Mater. Sci. Eng., A* **328**, 137 (2002).
- ¹⁷G. D. Hughes, S. D. Smith, C. S. Pande, H. R. Johnson, and R. W. Armstrong, *Scr. Metall.* **20**, 93 (1986).
- ¹⁸L. Lu, X. Chen, X. Huang, and K. Lu, *Science* **323**, 607 (2009).
- ¹⁹V. Yamakov, D. Wolf, S. R. Phillpot, A. K. Mukherjee, and H. Gleiter, *Philos. Mag. Lett.* **83**, 385 (2003).
- ²⁰H. Van Swygenhoven, P. M. Derlet, and A. G. Frøseth, *Nature Mater.* **3**, 399 (2004).
- ²¹H. J. Choi, S. W. Lee, J. S. Park, and D. H. Bae, *Jpn. Mater. Trans.* **50**, 640 (2009).
- ²²A. S. Khan, Y. S. Suh, X. Chen, L. Takacs, and H. Y. Zhang, *Int. J. Plast.* **22**, 195 (2006).
- ²³A. H. Chokshi, A. Rosen, J. Karch, and H. Gleiter, *Scr. Metall.* **23**, 1679 (1989).
- ²⁴J. Schiøtz, F. D. Di Tolla, and K. W. Jacobsen, *Nature* **391**, 561 (1998).
- ²⁵H. Conrad and J. Narayan, *Scr. Mater.* **42**, 1025 (2000).
- ²⁶A. S. Argon and S. Yip, *Philos. Mag. Lett.* **86**, 713 (2006).
- ²⁷H. Hahn and K. A. Padmanabhan, *Philos. Mag. B* **76**, 559 (1997).
- ²⁸H. Van Swygenhoven, M. Spaczer, A. Caro, and D. Farkas, *Phys. Rev. B* **60**, 22 (1999).
- ²⁹X. Li, Y. Wei, L. Lu, K. Lu, and H. Gao, *Nature* **464**, 877 (2010).
- ³⁰Z. X. Wu, Y. W. Zhang, and D. J. Srolovitz, *Acta Mater.* **59**, 6890 (2011).
- ³¹T. Narutani and J. Takamura, *Acta Metall. Mater.* **39**, 2037 (1991).
- ³²R. W. Armstrong and P. Rodriguez, *Philos. Mag.* **86**, 5787 (2006).
- ³³R. W. Armstrong, in *Mechanical Properties of Nanocrystalline Materials*, 1st ed., edited by J. C. M. Li (Pan Stanford, Singapore, 2011), p. 61.
- ³⁴H. Conrad, *Nanotechnology* **18**, 325701 (2007).
- ³⁵Y. M. Wang, A. V. Hamza, and E. Ma, *Acta Mater.* **54**, 2715 (2006).
- ³⁶M. Ames, M. Grewer, C. Braun, and R. Birringer, *Mater. Sci. Eng., A* **546**, 248 (2012).
- ³⁷L. Kurmanaeva, Yu. Ivanisenko, J. Markmann, K. Yang, H. J. Fecht, and J. Weissmüller, *Phys. Status Solidi RRL* **4**, 130 (2010).
- ³⁸D. S. Gianola, D. H. Warner, J. F. Molinari, and K. J. Hemker, *Scr. Mater.* **55**, 649 (2006).